

# Supporting Information

## Selective anisotropic growth of $\text{Bi}_2\text{S}_3$ nanoparticles with adjustable optical properties

Mariona Escoda-Torroella,<sup>1,2</sup> Carlos Moya,<sup>1,2,\*</sup> José A. Ruiz-Torres<sup>1,2</sup>, Arantxa Fraile Rodríguez,<sup>1,2</sup>  
Amílcar Labarta,<sup>1,2</sup> and Xavier Batlle<sup>1,2,\*</sup>

<sup>1</sup>Departament de Física de la Matèria Condensada, Martí i Franquès 1, 08028 Barcelona, Spain

<sup>2</sup>Institut de Nanociència i Nanotecnologia, Universitat de Barcelona, 08028 Barcelona, Spain

\*Corresponding author: [carlosmoyaalvarez@ub.edu](mailto:carlosmoyaalvarez@ub.edu), [xavierbatlle@ub.edu](mailto:xavierbatlle@ub.edu)

### Table of contents

**Figure S1.** Profiles of the reaction temperature for the series of samples  $S_{105}$  and  $S_{165}$ .

**Figure S2.** Particle size distributions of the series of samples  $S_{105}$  and  $S_{165}$ , obtained by transmission electron microscopy (TEM).

**Table S1.** Structural features of the series of samples  $S_{105}$  and  $S_{165}$ .

**Figure S3.** Selected area electron diffraction (SAED) pattern for sample  $S_{165}0$  indexed to the  $\text{Bi}_2\text{S}_3$  phase.

**Table S2.** Interplanar distances for sample  $S_{165}0$  computed from SAED images.

**Figure S4.** Multiple peak fitting of the X-ray diffraction spectra (XRD) for samples  $S_{105}120$  and  $S_{165}120$ .

**Table S3.** Crystal plane indexation and mean particle diameter obtained from XRD ( $D_{XRD}$ ) spectra for samples  $S_{105}120$  and  $S_{165}120$ .

**Figure S5.** Schematic illustration of the major planes in a  $\text{Bi}_2\text{S}_3$  nanorod (NR).

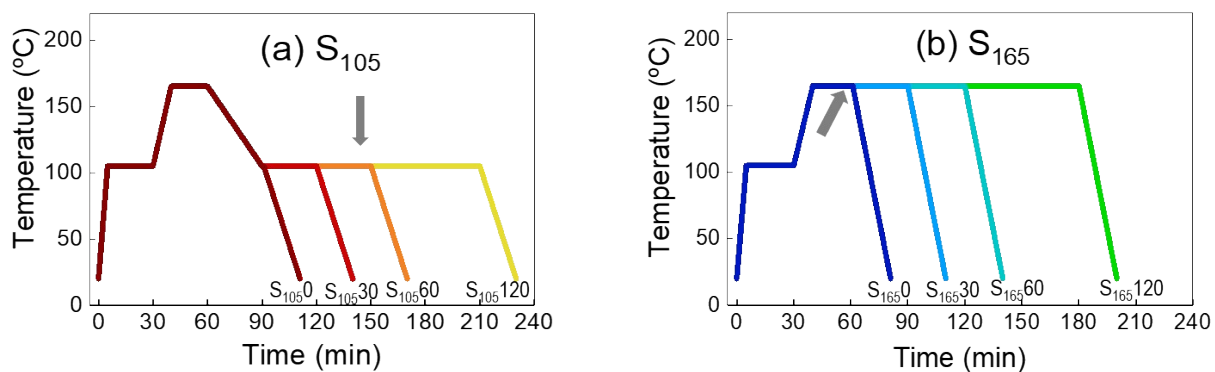


Figure S1. Reaction temperature profiles for series of samples (a)  $S_{105}$  and (b)  $S_{165}$ . Grey arrows are signaling the injection time of the thioacetamide mixture.

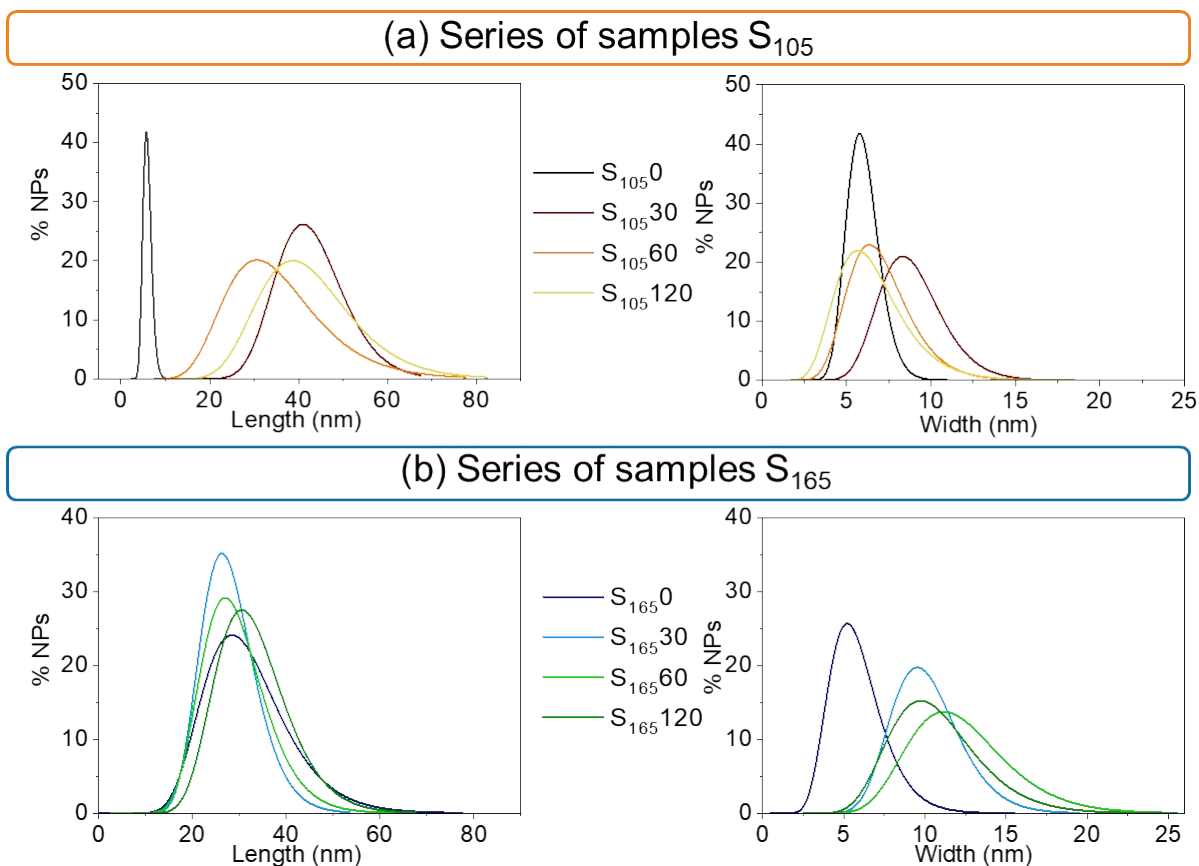


Figure S2. Particle length (left) and width (right) distributions obtained by fitting TEM histograms to log-normal distributions for the series of samples (a)  $S_{105}$  and (b)  $S_{165}$ , for times ranging from 0 to 120 min.

Sample	Morphology	Width (nm) $W_{TEM} \pm \sigma$ (RSD)	Length (nm) $L_{TEM} \pm \sigma$ (RSD)	Ratio (W:L)	$\eta$ (%)
S <sub>105</sub> 0	Spheroid	5.9 ± 0.8 (14%)	5.9 ± 0.8 (14%)	1:1	15.4
S <sub>105</sub> 30	Needle	8.9 ± 1.9 (21%)	43 ± 8 (19%)	1:5	21.5
S <sub>105</sub> 60	Needle	7.7 ± 1.4 (18%)	46 ± 6 (13%)	1:6	35.2
S <sub>105</sub> 120	Needle	6.0 ± 2.0 (33%)	43 ± 11 (26%)	1:7	43.7
S <sub>165</sub> 0	Rod	5.9 ± 1.7 (28%)	32 ± 9 (28%)	1:5	39.1
S <sub>165</sub> 30	Rod	10.2 ± 2.2 (22%)	28 ± 6 (21%)	1:3	45.9
S <sub>165</sub> 60	Rod	13 ± 3 (23%)	29 ± 7 (24%)	1:3	32.2
S <sub>165</sub> 120	Rod	11 ± 3 (26%)	33 ± 8 (24%)	1:3	41.0

Table S1. Structural and morphological parameters of the series of samples S<sub>105</sub> and S<sub>165</sub>, obtained from TEM images. RSD stands for relative standard deviation

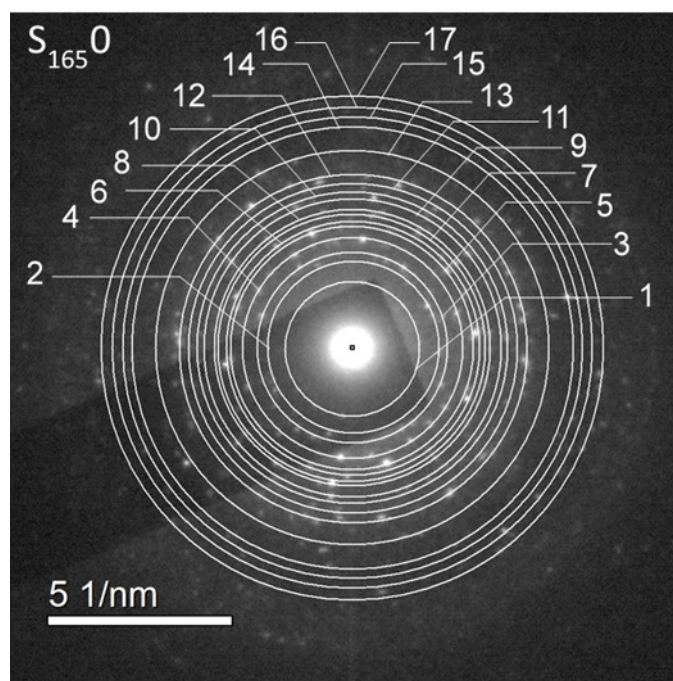


Figure S3. SAED pattern for sample S<sub>165</sub>0. Numbered rings are analyzed in Table S2 in the SI.

Sample	Ring	Experimental $d_{hkl}$ (Å)	$d_{hkl}$ (Å) $\text{Bi}_2\text{S}_3^1$	Plane of $\text{Bi}_2\text{S}_3^1$
<b>S<sub>105</sub>120</b>	1	5.55	5.5660	200
	2	3.93	3.9630	220
	3	3.81	3.7480	101
	4	3.33	3.2530	021
	5	3.01	3.1100	211
	6	2.89	2.8240	040
	7	2.75	2.7170	301
	8	2.66	2.6410	311
	9	2.45	2.4560	231
	10	2.38	2.3050	041
	11	2.18	2.1880	510
	12	2.12	2.1180	421
	13	2.07	2.0750	520
	14	1.661	1.6650	611
	15	1.59	1.5870	550
	16	1.538	1.5328	720
	17	1.46	1.4809	271

Table S2. Interplanar distances for sample S<sub>165</sub>0 computed from the SAED pattern in Fig. S3 in the SI, using the Bi<sub>2</sub>S<sub>3</sub> reference code: 00-017-0320.

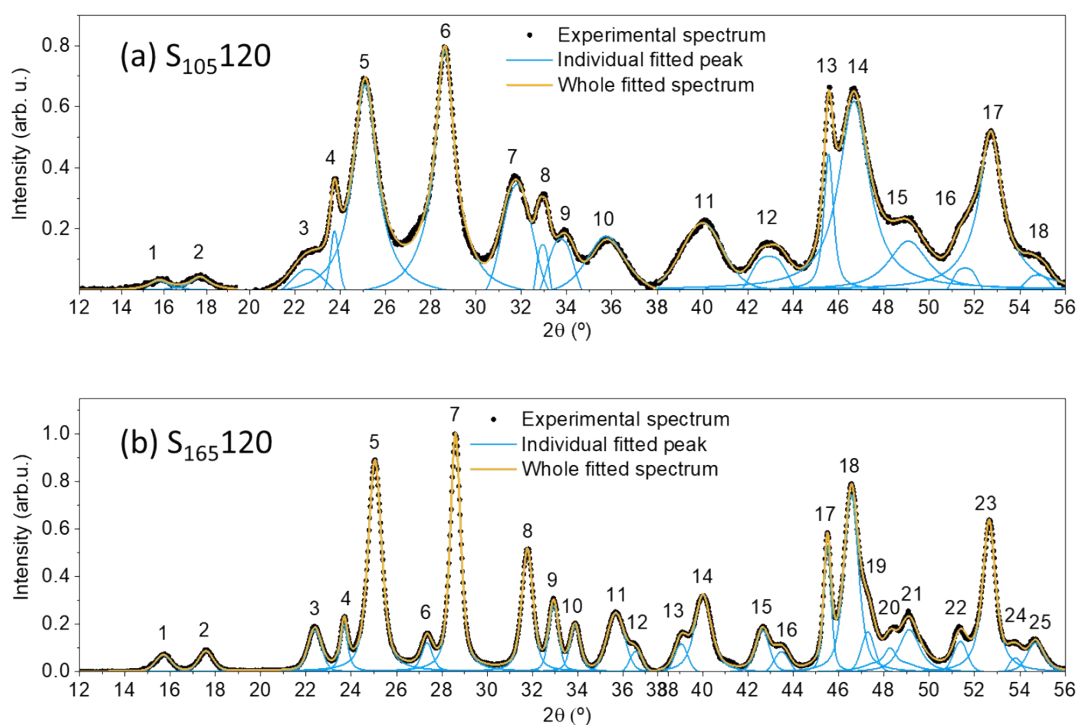


Figure S4. Multiple peak fitting of the XRD spectra from 12 to 56° for the samples S<sub>105</sub>120 (a) and S<sub>165</sub>120 (b). For each sample, the experimental spectrum (black spheres), whole fitted spectrum (yellow solid line), and individual fitted peaks (blue solid line) are depicted. Numbered peaks are analyzed in Table S3 in the SI.

$S_{105}120$				$S_{165}120$			
Peak	$2\theta$ (°)	$D_{XRD}$ (nm)	Plane	Peak	$2\theta$ (°)	$D_{XRD}$ (nm)	Plane
1	15.76	7.2	200	1	15.70	10.5	020
2	17.70	7.3	120	2	17.59	11.2	120
3	22.57	5.0	220	3	22.39	12.2	220
4	23.75	18.9	101	4	23.69	22.9	101
5	25.10	6.5	310	5	25.05	12.1	130
6	28.62	8.0	211	6	27.35	14.9	021
7	31.82	5.7	221	7	28.60	16.0	211
8	32.94	15.0	301	8	31.78	14.7	221
9	33.74	7.1	311	9	32.93	17.1	301
10	35.75	4.1	240	10	33.88	16.4	311
11	40.01	4.2	430	11	35.69	9.7	240
12	42.94	5.7	250	12	36.57	14.2	231
13	45.56	18.0	002	13	39.05	13.1	041/141
14	46.68	5.6	501	14	40.01	10.2	430
15	49.08	4.5	160	15	42.65	12.5	421
16	51.58	8.7	222	16	43.48	11.8	250/520
17	52.72	7.3	312/061	17	45.51	23.4	002
18	54.78	8.6	161	18	46.56	11.9	431/501
				19	47.30	13.1	530
				20	48.27	10.1	060
				21	49.12	8.4	160
				22	51.37	12.6	222
				23	52.64	13.6	351
				24	53.80	15.0	061
				25	54.69	10.7	360

Table S3. Plane indexation and  $D_{XRD}$  for samples  $S_{105}120$  (left) and  $S_{165}120$  (right) obtained from the multiple peak fitting of the XRD spectra in Fig. S4 in the SI.

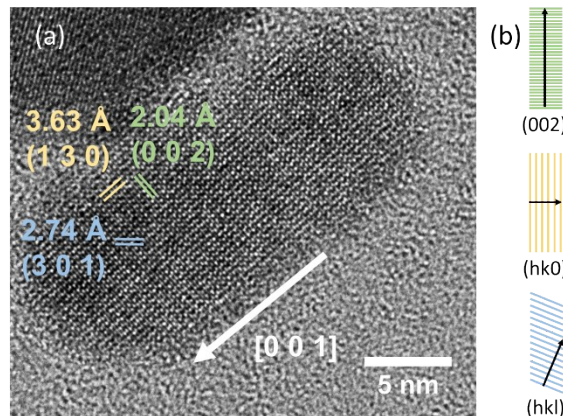


Figure S5. (a) Main interplanar distances together with their corresponding planes for a single  $\text{Bi}_2\text{S}_3$  NR of sample  $S_{165}120$ . (b) Schematic illustrations of perpendicular (002), parallel (hk0), and diagonal (hkl) planes. Crystal growth along the [001] direction is shown with a white arrow.